# Effect of Communication Delays on the Successful Coordination of a Group of Biomimetic AUVs

Jonathan McColgan
Division of Aerospace Science
School of Engineering
University of Glasgow
Glasgow, G12 8QQ

Euan W. McGookin
Division of Aerospace Science
School of Engineering
University of Glasgow
Glasgow, G12 8QQ

*Abstract*— **In this paper, the influence of delays on the ability of a formation control algorithm to coordinate a group of twelve Biomimetic Autonomous Underwater Vehicles (BAUVs) is investigated. In this study the formation control algorithm is a decentralized methodology based on the behavioural mechanisms of fish within school structures. Incorporated within this algorithm is a representation of the well-known and frequently used communication protocol, Time-Division-Multiple-Access (TDMA). TDMA operates by assigning each vehicle a specific timeslot during which it can broadcast to the remaining members of the group. The size of this timeslot varies depending on a number of operational parameters such as the size of the message being transmitted, the hardware used and the distance between neighbouring vehicles. Therefore, in this work, numerous timeslot sizes are tested that range from theoretical possible values through to values used in practice. The formation control algorithm and the TDMA protocol have been implemented within a validated mathematical of the RoboSalmon BAUV designed and manufactured at the University of Glasgow. The results demonstrate a significant deterioration in the ability of the formation control algorithms as the timeslot size is increased. This deterioration is due to the fact that as the timeslot size is increased, the interim period between successive communication updates increases and as a result, the error between where the formation control algorithm estimates each vehicle to be and where they actually are, increases. As a result, since the algorithm no longer has an accurate representation of the positioning of neighbouring vehicles, it is no longer capable of selecting the correct behavioural equation and subsequently, is unable to coordinate the vehicles to form a stable group structure.**

***Keywords—formation control algorithms, mathematical modelling, biomimetic, schooling***

## I. INTRODUCTION

Oceanography can be described as the collection of data associated with the chemical [1], geological [2] and physical [3] processes of the Earth's Oceans. At present, the majority of oceanography is completed using a class of submersibles known as Autonomous Underwater Vehicles (AUVs). These vehicles, with their ability to house extremely sophisticated sensor packages and travel to any required depth, have revolutionised the collection of oceanographic data [4]. While current AUV missions usually consist of a single vehicle following a predefined trajectory [5], in the future it is envisioned that multiple AUVs will be deployed as part of a group [6] acting as a mobile sensor network [7]. In doing so, these groups would be capable of collecting data over spatiotemporal scales presently not achievable through the use of a single vehicle [8]. Therefore, due to these significant operational benefits, it is unsurprising that a large proportion of research within the AUV community over the past decade has been focussed on investigating the feasibility of deploying a group of AUVs [9].

To date, these studies have been focussed on investigating the deployment of groups of traditional AUVs. These conventional designs can be characterised by a cylindrically shaped hull for hydrodynamic performance, a propeller or buoyancy driven propulsion method and control surfaces for manoeuvrability [10], [11] [12]. However, in the past two decades a number of studies have involved the development of a new class of underwater vehicle known as Biomimetic Autonomous Underwater Vehicles (BAUVs) [13], [14].

As the name suggests, BAUVs mimic the propulsive and steering mechanisms of real aquatic creatures (e.g. fish) to produce a vehicle that is not only more efficient at low speeds but also possesses superior manoeuvrability characteristics [13], [15], [16] These unique characteristics provide BAUVs with operational capabilities that traditional AUVs do not have, e.g. being able to operate within confined spaces. Furthermore, these vehicles can be designed and manufactured at a fraction of the price of traditional AUVs and as a result, are particularly suited to be operated within a multi-vehicle deployments [17].

However, before such multi-vehicle collaboration can occur, a guidance heuristic has to be implemented that will allow the individual vehicles to firstly communicate with one another and then coordinate themselves into a specific formation. However, as a result of the Earth's watery veil providing a barrier through which no radio waves can propagate, vehicles operating underwater do so in an environment whereby the communication channel is characterized by low bandwidth and large delays [18]. Consequently, the implementation of formation control algorithms to underwater vehicles presents a number of unique challenges not faced in the air, land and space domains.

Consequently, it is the aim of this paper to investigate to what extent these communicative limitations influence the ability of a formation control algorithm to enable a group of AUVs to coordinate themselves and form a stable group structure. To achieve this, the work completed in this research will utilize a validated mathematical model of the biomimetic AUV, RoboSalmon, which has been designed and manufactured at the University of Glasgow. Incorporated into this model is a formation control algorithm based on the behavioural mechanisms of fish partaking in schooling behaviour. The implementation and accompanying analysis detailing the necessary conditions to ensure the vehicles are able to coordinate themselves using this particular algorithm are discussed in detail in [19].

The focus of this paper is concerned with the alterations needed to be made to these algorithms in order to accommodate realistic communication delays. This is achieved by incorporating an accurate representation of the underwater communication channel in the form of a suitable communication protocol. The particular protocol chosen is referred to as the Time-Division-Multiple-Access (TDMA) protocol which is utilized frequently in the underwater domain and operates by assigning each vehicle within the group a specific timeslot during which it can broadcast to the remaining members of the group [20]. Once each vehicle has communicated once, the process repeats itself and continues to do so until the end of the mission.

The length of the particular timeslot is based on a number of parameters including the transmission time of the message being sent, the propagation delay and a parameter known as the guard time which is incorporated to improve the reliability of the protocol [21]. Although theoretical values can be calculated for these parameters, the values obtained vary quite significantly from those obtained in real-life. Therefore, for the work contained within this paper, both theoretically possible values as well as values utilised in practice are incorporated and their influence analyzed.

This paper presents the details of the study in the following manner. Section II presents a brief overview of the RoboSalmon vehicle and the associated mathematical model. Section III describes the implementation of the formation control algorithm utilised, as well as the incorporation of the TDMA communication protocol. Section IV describes the scenarios simulated, the results obtained and the corresponding analysis. Finally, Section V concludes the paper with the findings of the study.

## II. RoboSalmon AUV and Mathematical Model

As the design of the RoboSalmon vehicle (Figure 1) is based on the North Atlantic salmon, it utilises between fifty and sixty percent of its total body length to generate the required propulsive wave associated with fish locomotion. This particular species of fish has been chosen due to its swimming characteristics allowing it to be both fast in a straight line as well as extremely manoeuvrable while turning [22].

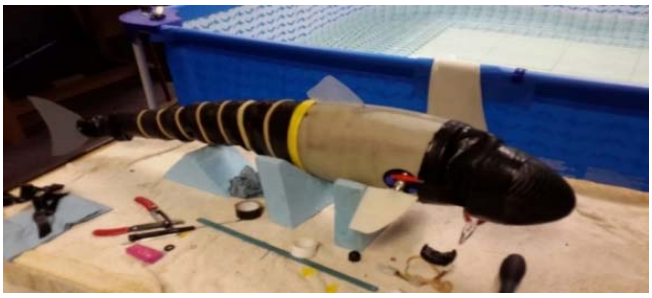

Figure 1 - RoboSalmon BAUV

The RoboSalmon vehicle is capable of replicating the swimming gait of the North Atlantic due to the coordinated movement of the vehicle's fully actuated tail section [23]. Consequently, the vehicle is extremely maneuverable with a turning radius of less than one body length and a straight line speed of 0.15m/s.

### A. Mathematical Model

The dynamics of the RoboSalmon vehicle can be represented within a mathematical model using the state-space form shown below [23].

$$\begin{bmatrix}\dot{\boldsymbol{\nu}}\\ \dot{\boldsymbol{\eta}}\end{bmatrix} = \begin{bmatrix}\mathbf{M^{-1}}\left(-(\mathbf{C}(\boldsymbol{\nu})+\mathbf{D}(\boldsymbol{\nu})+\mathbf{g}(\boldsymbol{\eta})\boldsymbol{\nu}^{-1})\right)\\ \mathbf{J}(\boldsymbol{\eta})\end{bmatrix}\begin{bmatrix}\boldsymbol{\nu}\\ \boldsymbol{\eta}\end{bmatrix} + \begin{bmatrix}\mathbf{M^{-1}}\\ \mathbf{0}\end{bmatrix}\boldsymbol{\tau} \quad (1)$$

This contains the Rigid Body Dynamics (upper matrix equation) and the kinematic transformations to the Earth-fixed reference frame (lower matrix equation). In the Rigid Body Dynamics **M** is the mass/inertia matrix, **C** is the Coriolis matrix, **D** is the damping matrix, $\boldsymbol{\nu}$ is the state vector containing the Body-Fixed velocities and $\boldsymbol{\tau}$ is the input force/moment vector [25]. It should be noted that the gravitational force/moment vector, **g** , is zero due to the assumption of neutral buoyancy. In the kinematic expression $\boldsymbol{\eta}$ represents the Earth-Fixed dynamic variables (Earth Fixed position and orientation) and **J** is the Euler kinematic transformation matrix [24].

Only longitudinal, lateral and yawing dynamics are consider and as a result, six states are represented within the model as shown in Table 1.

Table 1 - Body-Fixed & Earth-Fixed Parameters

| Body Fixed Velocities | Parameter | Earth Fixed Variables | Parameter |
|---|---|---|---|
| Surge | $u$ | X-Coordinate | $x_e$ |
| Sway | $v$ | Y-Coordinate | $y_e$ |
| Yaw | $r$ | Heading Angle | $\psi$ |

## III. Formation Control Algorithm

In order to deploy a self-organizing group of BAUVs, the formation control algorithms have to ensure that neighbouring vehicles do not collide with one another and that the vehicles are suitably spaced to ensure the maximum area is mapped. To satisfy these requirements, the work presented in this paper takes inspiration from nature and utilizes the behavioural mechanisms of fish within school structures [25].

As shown below in Figure 2, these mechanisms operate by associating a number of behavioural zones to each vehicle and depending on which of the zones is occupied, the vehicle will manoeuvre in either an *attractive, orientating* or *repulsive* manner [26]–[28].

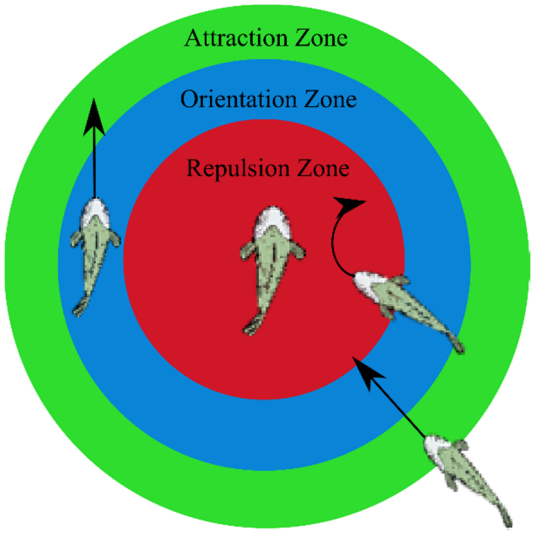


Figure 2 - Behavioural Zones of Fish within School Structure

It is apparent from Figure 2 that in order for each vehicle to determine which of its three behavioural zones is occupied, each member of the group needs to know the positional data of the other members of the group. Furthermore, when the orientating behaviour is utilised, each vehicle also needs to know the heading angle of its nearest neighbours. Consequently, it is these three parameters that each vehicle transmits during their assigned timeslot in the TDMA protocol.

However, before the above mechanism can be implemented as a formation control strategy, it is important to understand the structure of the vehicle's guidance system.

### *A. RoboSalmon Guidance System*

The structure of the guidance system utilised within the RoboSalmon vehicle is presented below in Figure 3.

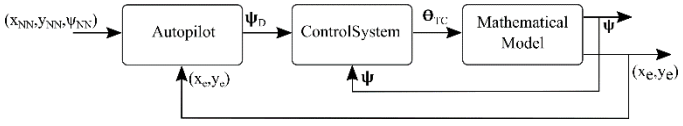


Figure 3 - Guidance System Structure

As shown above, the guidance system comprises of two subsystems: the *autopilot* and the *control system*. The autopilot calculates the desired heading angle of the vehicle, $\psi_D$ and the control system utilizes the difference between the desired and current heading angle of the vehicle to evaluate the required caudal fin deflection, $\theta_{TC}$ that is required to manoeuvre the vehicle to the required heading angle. The control system used to evaluate this angle is a PI controller that can be represented by the following equation [23]:

$$\theta_{TC} = K_p \Delta\psi + K_i \int \Delta\psi \, dt \tag{2}$$

Here, $K_p$ and $K_i$ are the proportional and integral gains that are equal to $3.4\text{x}10^{-2}$ and $2\text{x}10^{-5}$ respectively and $\Delta\psi$ is difference between the desired and current heading angle of the vehicle.

### *B. Behavioural Equations*

Based on the structure of the guidance system, it is apparent that in order to implement the behavioural mechanisms discussed above, the Autopilot will have to produce a desired heading angle that results in each vehicle maneuvering in either a repulsive, attractive or orientating manner. Implementation of each of these is discussed below.

#### *1) Attractive Behavioural Equation*

The attractive behavioural equation has to ensure that each vehicle manoeuvres to reduce the distance to its nearest neighbour(s). To achieve this, a waypoint is generated which is equal to the average position of the vehicles nearest neighbour(s) as shown below in Equations (3) & (4).

$$x_d = \frac{1}{I_{NN}} \sum_{NN=1}^{I_{NN}} x_{NN} \tag{3}$$

$$y_d = \frac{1}{I_{NN}} \sum_{NN=1}^{I_{NN}} y_{NN} \tag{4}$$

Here $x_{NN}$ and $y_{NN}$ are the x and y positions of the AUVs nearest neighbours and $I_{NN}$ is the number of neighbours taken into consideration. The coordinate calculated by the above equations is then used to evaluate the desired heading angle of the vehicle using the equation below.

$$\psi_D = tan^{-1}\left(\frac{y_d - y_e}{x_d - x_e}\right) \tag{5}$$

Here $x_e$ and $y_e$ is the current position of the vehicle whose heading angle is being calculated.

#### *2) Orientating Behavioural Equation*

The purpose of the orientating behavioural equation is to ensure that all the vehicles within the group manoeuvre with the same heading angle. Therefore, if a vehicle's nearest neighbour occupies its orientation zone, the desired heading angle of the vehicle is simply the average heading angle of the group. In this zone Equation (6) is used to calculate the desired heading:

$$\psi_D = \frac{1}{I_{NN}} \sum_{NN=1}^{I_{NN}} \psi_{NN} \tag{6}$$

*3) Repulsive Behavioural Equation*

Finally, the repulsive behavioural equation has to ensure that neighbouring vehicles maintain a minimum separation distance. This is achieved by implementing the following conditional statement.

$$\psi_D = \begin{cases} \psi_{ref} + \left(\frac{NN_L}{NN_L + NN_R}\right)\frac{\pi}{2} & ,if\ NN_L > NN_R \\ \psi_{ref} - \left(\frac{NN_L}{NN_L + NN_R}\right)\frac{\pi}{2} & ,if\ NN_L \leq NN_R \end{cases} \quad (7)$$

Here $\psi_{\text{ref}}$ is the desired heading angle of the group, $NN_L$ and $NN_R$ is the number of nearest neighbours to left and right of the vehicle respectively.

*C. Algorithm Structure*

However, before utilizing any of the above equations, the autopilot must go through the process of deciding what zones are occupied by its nearest neighbours and therefore, which behavioural equation to utilize. This process of deciding which behavioural zone is occupied and the subsequent evaluation of the demanded heading angle is known as the *algorithm structure* and is presented below in Figure 4.

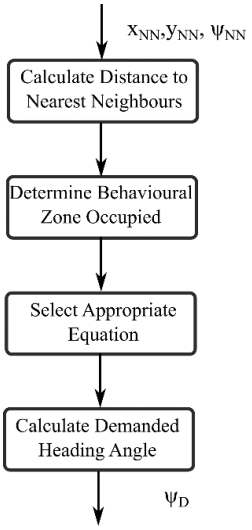


Figure 4 - Algorithm Structure

The process presented in Figure 4 occurs within the Autopilot subsystem of Figure 3 and as such, is evaluated at the same rate as the guidance system. For the work presented in this paper, the update rate is set to 4Hz. Also, if multiple zones are occupied, priority is given to the zone closest to the vehicle.

Therefore, the above section has described the equations and algorithmic structure utilised to produce a formation control algorithm based on the behavioural mechanisms of fish within school structures. This algorithm, as highlighted in [19], has demonstrated that under the assumption of instantaneous communication and as long as at least six nearest neighbours are taken into consideration, it is capable of guaranteeing the formation of a stable group structure.

However, as previously mentioned, the assumption of instantaneous communication is not realistic, particularly in the underwater domain. In order to rectify this, a suitable communication protocol has to be incorporated into the algorithms as outlined below.

*D. Communication Protocol*

As discussed above, the work presented in this paper involves the implementation of the TDMA protocol. This protocol operates by assigning each vehicle within a group a unique timeslot during which it can transmit data to the other vehicles. Once each vehicle has transmitted its data once, the process is repeated and the cycle continues until the end of the mission.

The length of the timeslot, $T_{Tot}$ is dependent on three factors: the transmission time of the data, the propagation delay due to the speed of sound in water and a user defined safety factor known as the *Guard Time*. Using these three parameters, the timeslot can be calculated using the following equation:

$$T_{Tot} = T_T + T_P + T_G \quad (8)$$

Where $T_T$ represents the transmission time, $T_P$ is the propagation delay and $T_G$ is referred to as the guard time.

*1) Transmission Time*

The magnitude of $T_T$ is based on the size of the message being sent and the transmission rate of the modem. As discussed above, the only parameters required to allow the formation control algorithms to operate are the coordinates and heading angle of each member of the group. Subsequently, the size of each message being sent is relatively small as shown below in Table 2.

Table 2 - Contents & Size of Message

| Parameter | Size (bytes) |
|---|---|
| Vehicle ID | 2 |
| X-Coordinate | 4 |
| Y-Coordinate | 4 |
| Z-Coordinate | 4 |
| Heading Angle | 4 |

Therefore, assuming the transmission rate of the modem is 31.2kbits/s, the 18 byte message shown above has a transmission time of approximately 0.005s.

*2) Propagation Delay*

The propagation delay represents the time taken for the message to travel from the transmitting vehicle to the receiving vehicle(s). Therefore, this parameter is evaluated by dividing the distance between the relevant vehicles by the speed of sound in water (1500 m/s). However, as it is not possible to know the exact value of this distance, a conservative estimate, which is equal to the time taken for the data to be transferred across the maximum range of the acoustic modem can be used.

*3) Guard Time*

The guard time is included within the TDMA protocol as a precaution to reduce the likelihood of successive broadcasts

colliding and leading to the loss of data at the receiving vehicle(s). The magnitude of this parameter is calculated using the equation showing below.

$$T_G = \beta T_P \quad (9)$$

Where $\beta$ is a user defined parameter set to one in this instance and $T_P$ is the propagation delay.

By evaluating and combining these three parameters, an estimate for the timeslot size that will ensure the various vehicles within the group are able to communicate efficiently can be obtained. Moreover, it is apparent that the dominating parameter in deciding the timeslot size is the propagation delay which as discussed above, is itself, based on the maximum range of the acoustic modem used within the vehicle.

Subsequently, with acoustic modems now available with a maximum range anywhere in the region between 350m and 8 km, the associated timeslot size will vary significantly. More precisely, the timeslots associated with the above figures will be equal to 0.5s and 10.7s respectively. However, figures quoted in the literature suggest that in reality that value can vary anywhere between 6s and 30s [29]–[32].

### *E. Incorporating Communication Protocol*

Finally, to incorporate the TDMA protocol, the formation control algorithms have been altered to incorporate a delay in the rate at which each vehicle receives an update from the other members of the group. This is shown below in Figure 5.

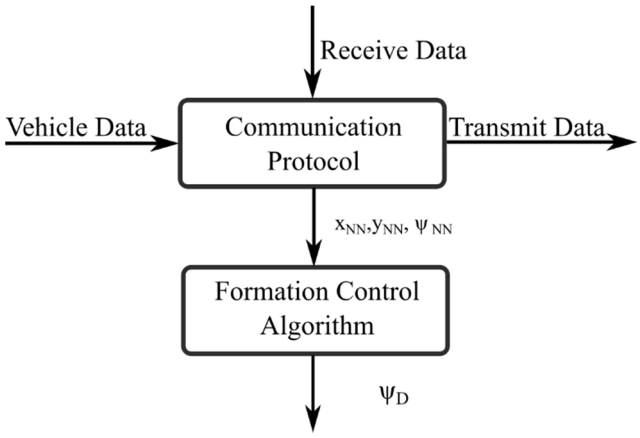


Figure 5 - Algorithm Structure with Communication Protocol Incorporated

With the TDMA protocol now incorporated, the formation control algorithm will only receive positional updates at the discrete intervals marked by the beginning of each timeslot. Furthermore, due to the fact that only one member of the group is able to transmit during these intervals, the time taken for every member of the group to communicate once (communication cycle length) is equal to the timeslot size multiplied by the size of the group. For example, a timeslot size of 0.5s results in each vehicle receiving a new message every 0.5s but only after six seconds, will it receive an update from its nearest neighbour.

Therefore, it is the aim of this paper to determine to what effect the timeslot size has on the ability of the formation control algorithm to enable a group of 12 biomimetic AUVs to form a stable group structure. A stable group structure is defined as the ability of the formation control algorithm to ensure that all 12 vehicles converge towards utilizing the orientating behaviour continuously.

### *F. Simulation Scenario & Setup*

As the purpose of this investigation is to analyze the effect of increasing the timeslot size, simulations have been completed that allowed the value for this parameter to be varied from half a second through to twenty-four seconds. These limits have been chosen to ensure that both the theoretically possible values, as well as the more realistic values are investigated. Furthermore, for each of the timeslot sizes, 100 simulations have been performed that varied the initial positions of the 12 vehicles.

Also, the formation control algorithms have been deemed to be successful if all 12 vehicles within the group converged to utilizing the orientating behaviour exclusively and continuously for at least one minute. This ensures the formation of the aforementioned stable group structure is obtained.

Finally, the particular scenario simulated is based on the envisioned future of oceanographic missions as described in [6]. This scenario involves multiple vehicles being deployed from a surface vessel before using a formation control algorithm similar to that described above to produce a formation that maximizes sensor coverage. To mimic this scenario, the initial positions of the vehicles have been specifically chosen to ensure that the vehicles are all in close proximity to one another as they would be if they had been deployed from a surface vessel. Furthermore, the size of the behavioural zones are chosen to be sufficiently large to ensure the vehicles would all initially have to use the repulsive behavioural equation and thus move apart to maximize sensor coverage. A summary of these simulation parameters are presented below in Table 3.

Table 3 - Simulation Parameters

| Parameter | Value |
|---|---|
| Behaviour Zone Size | [20,25,200]m |
| Number of Vehicles | 12 |
| Timeslot Size | [0.5,1,2,4,8,16,24]s |
| Simulations per Timeslot | 100 |

## IV. RESULTS

To demonstrate the effect that introducing the aforementioned communication protocol and increasing the associated timeslot size has on the effectiveness of the formation control algorithms, shown below in Figures 6 (a) – (d) are the trajectories obtained as the timeslot size is increased from zero (instantaneous communication) through to eight seconds.

The results presented in Figures 6 have been obtained from just one of the 100 simulations completed for each timeslot size but

as will be shown below, the results are representative of the typical trajectories obtained across all simulations.

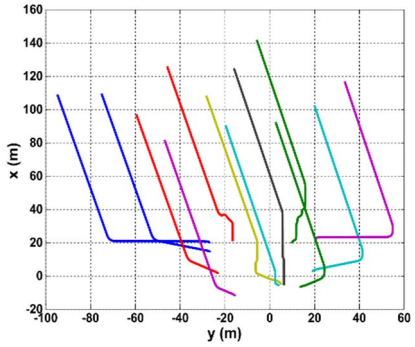


(a) Instantaneous Communication

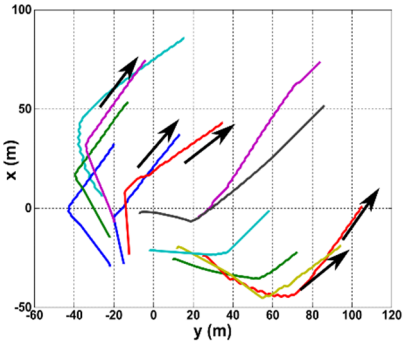


(b) Timeslot = 2s

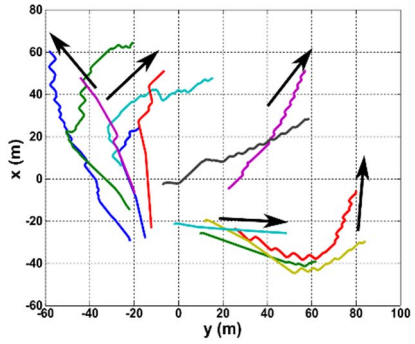


(c) Timeslot = 4s

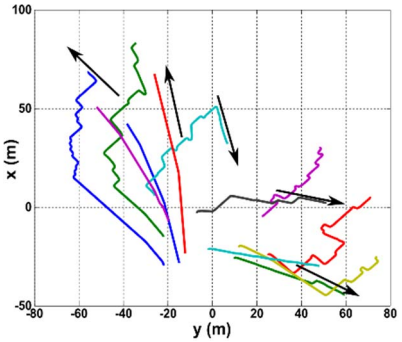


(d) Timeslot = 8s

Figure 6 – Vehicle Trajectories as Timeslot Size is Increased.

It is apparent from Figure 6(a) that when instantaneous communication is assumed, the formation control algorithms are capable of promoting the formation of a stable group structure. However, as the communication protocol is implemented and the associated timeslot size increased, Figures 6(b) – (d) demonstrate that the algorithms become less and less effective and the number of vehicles capable of converging towards a common heading angle decreases.

Before the reasons why the algorithms become less effective can be understood, it is important to firstly understand the mechanisms that result in the formation of stable group structure when instantaneous communication is assumed. To achieve this, the results obtained from these particular simulations are analyzed and discussed in the following section.

### *A. Ideal Commuication*

As shown in Figure 4, the mechanism within the formation control algorithm that decides which behavioural equation to use is the distance between each vehicle and its nearest neighbour. As discussed in the previous section, the initial value for this parameter has been chosen to be specifically less than the lower boundary of the orientation zone, i.e. less than 20m. As a result, it is expected that each vehicle within the group will initially utilize the repulsive behavioural equation. Subsequently, as the vehicles begin to coordinate, the distance between each vehicle and its nearest neighbour will begin to increase. As this occurs, the number of vehicles within each group utilizing the orientating behaviour should also begin to increase and as a result, the vehicles will begin to converge towards a common heading angle.

To demonstrate that this is indeed what happens, the evolution of the distance between each vehicle and its nearest neighbour, the number of vehicles utilizing the different behavioural equations and finally, the standard deviation of the vehicles heading angle are presented below in Figure 7. The results presented represent the average values obtained across the 100 simulations completed.

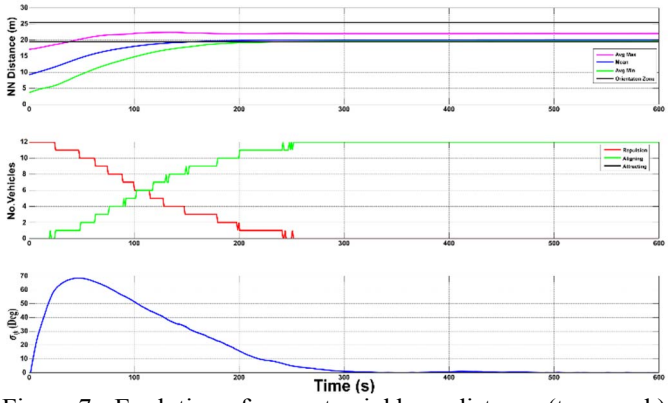


Figure 7 - Evolution of nearest neighbour distance (top graph), number of vehicles utilizing different behavioural equation (middle graph), standard deviation of heading angle (bottom graph)

The results clearly demonstrate the desired behaviour and demonstrate that when instant communication is assumed, the formation control algorithms are capable of coordinating a

group of AUVs to form a stable group structure moving with a common directionality and at a specified nearest neighbour distance.

*B. Communication Protocol Incorporated*

However, as shown in Figures 6(b)-(d), as soon as the communication protocol is incorporated, the ability of the formation control algorithm to successfully coordinate the vehicles begins to decrease. In order to understand why this is the case, it is important reemphasize that because the TDMA protocol has been implemented, each vehicle will only have an accurate representation of its nearest neighbour's position once every communication cycle. Therefore, in the interim period between successive communication updates, each vehicle will utilize the previous communicated position of its nearest neighbour to calculate the distance between the two vehicles. As a result, an error between where each vehicle estimates its nearest neighbour to be and where it *actually* is will appear. In order to understand how this error is affected by an increase in the timeslot size, Figure 8 represents the evolution of this parameter for the various timeslot sizes simulated. Again, the results presented below represent the average value calculated across the 100 simulations completed at each timeslot size.

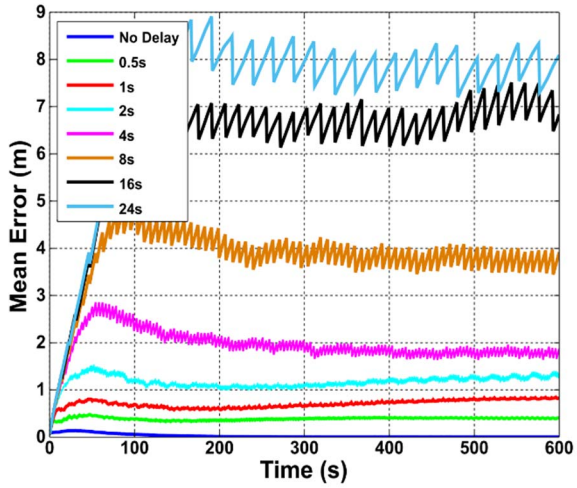


Figure 8 - Nearest Neighbour Distance Error

Unsurprisingly, the results demonstrate that as the timeslot size increases, the magnitude of the error increases. However, the results also demonstrate that the error appears to be cyclical in nature with a decrease in frequency occurring as the timeslot size increases. This behaviour is due to the fact that as the timeslot size increases, the period between successive communication updates, i.e. the communication cycle length also increases and as a result, the frequency at which each vehicle receives a positional update from its nearest neighbour decreases.

While the results presented in Figure 8 describe the evolution of the error and how it is affected by variations in the timeslot size, they fail to explain exactly why the incorporation of the communication protocol prevents the formation control algorithm from successfully coordinating the vehicles as shown in Figure 6.

Therefore, in order to understand why this is the case, it is necessary to relate the errors discussed above in Figure 8 with the evolution of the estimated nearest neighbour distance as calculated within the formation control algorithm during the interim period between communication updates. This is shown below in Figure 9 for a timeslot size of 0.5s.

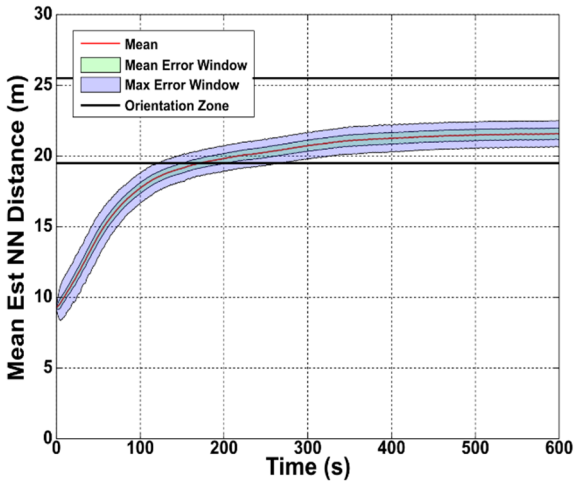


Figure 9 - Estimate of Nearest Neighbour Distance and Associated Mean and Maximum Error for a Timeslot Size of 0.5s

In the above figure, the red line represents the evolution of the estimated nearest neighbour distance as evaluated within the formation control algorithm averaged across the 100 simulations completed. Subsequently, it represents the nearest neighbour distance utilised within the formation control algorithm to select the relevant behavioural equation. The shaded areas meanwhile represent the average maximum and mean errors associated with this estimation. Consequently, although the majority of vehicles will have used a nearest neighbour distance similar to that represented by the red line, the true nearest neighbour distance will be anywhere within the shaded regions.

As a result, due to this error, it is now likely that the formation control algorithm will select the incorrect behavioural equation. This is demonstrated in Figure 9 where, in the period between 130s and 260s, the shaded area is within both the orientation and repulsion zones. This means that in some instances, the vehicles estimate of its nearest neighbour distance will result in it utilizing the repulsive behavioural equation when in reality, it should be using the orientating behavioural equation and vice versa.

Therefore, based on the results presented in Figure 9, the communication delay resulting from incorporating a realistic communication protocol is likely to result in the formation control algorithms selecting the incorrect behavioral equation. Furthermore, while the results presented in Figure 9 are only representative of those obtained when the timeslot size is equal to 0.5s, the fact that the magnitude of the error increases as the timeslot size does (Figure 8), it is anticipated that the number of vehicles utilizing the incorrect behaviour will only increase

as the timeslot size does. To demonstrate that this is the case, shown below in Figure 10 is the evolution of the percentage of vehicles utilizing the wrong behavioural equation for the various timeslot sizes.

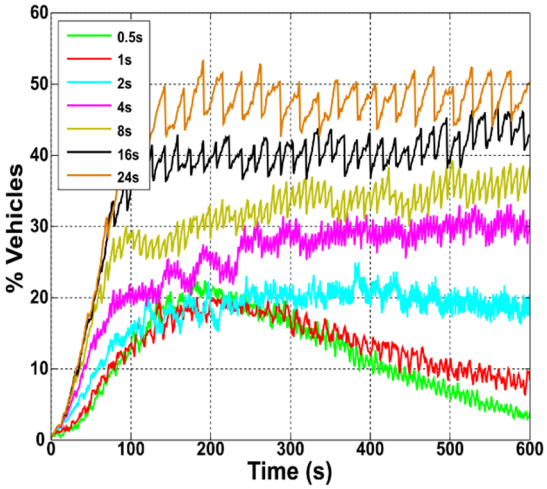


Figure 10 - Percentage of Vehicles Utilising the Wrong Behavioural Equation as the Timeslot Size is Increased

The results are as expected, with an increase in the percentage of vehicles utilizing the wrong behavior occurring as the timeslot size is increased. Furthermore, as with Figure 8, the results appear to be oscillatory in nature. This oscillatory behaviour can be explained by the results presented in Figures 8 & 9 whereby in the interim period between successive communicate updates, each vehicle, as a result of the error shown in Figure 8, will select the wrong behavioural equation (Figure 9). Consequently, the percentage of vehicles utilizing the wrong behaviour will increase throughout the communication cycle as shown in Figure 10. However, at the start of each timeslot, at least one vehicle from each group will receive an update from its nearest neighbour and as a result, will be momentarily capable of selecting the correct behaviour. Subsequently, as shown in Figure 10, this will lead to a reduction in the number of vehicles utilizing the wrong behavioural equation. Due to the cyclical nature of the TDMA protocol, this process of utilizing the wrong behavioural equation before being corrected during a subsequent communication update will occur continuously and explains the oscillatory nature of the results presented in Figure 10.

As a result of continuously oscillating between the correct and incorrect behaviors, the formation control algorithms will also be continuously switching between utilizing either the repulsive, orientating and attractive behaviors. As a result, the ability of the algorithms to converge towards utilizing the orientating behaviour exclusively will be compromised. Furthermore, based on the fact that the percentage of vehicles selecting the incorrect behavior increases with the timeslot size, a subsequent decrease in the percentage vehicles capable of converging toward utilizing the orientating behaviour should be expected. This is demonstrated to be the case in Figure 11 where the variation in the percentage of vehicles capable of converging towards utilizing the orientating behaviour is presented.

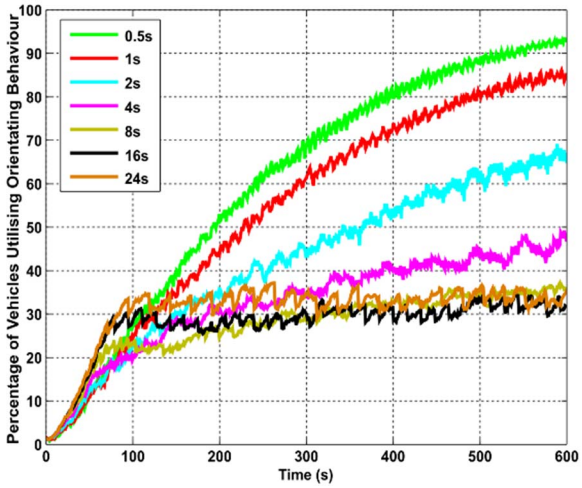


Figure 11 - The Evolution of the Percentage of the Number of Vehicles Utilising either the Orientating Behavioural Equations.

The results presented above are as expected, with a significant decrease in the percentage of vehicles utilizing the orientating behavior as the timeslot size is increased. Subsequently, as discussed above, if the vehicles aren't utilising the orientating behaviour, they must be using either the repulsive or attractive behaviours. Consequently, since these equations are designed to manoeuvre the vehicles in opposing directions, it is to be expected that as less vehicles utilize the orientating behaviour, the resulting group formation will include vehicles maneuvering in significantly different directions. This is shown to be the case below in Figure 12, where the evolution of the standard deviation of the vehicle's heading for the various timeslot sizes is presented.

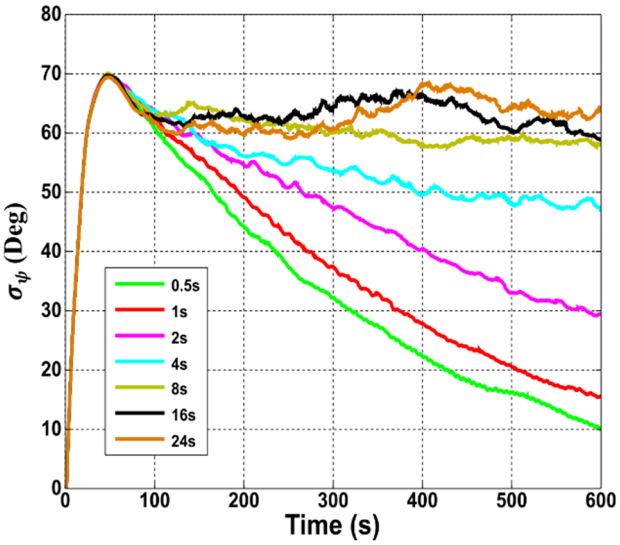


Figure 12 - Evolution of the Standard Deviation of the Group Heading Angle for Various Timeslot Sizes

Again, the results presented in Figure 12 are as expected with an increase in the standard deviation occurring as the timeslot

size is increased. These results agree with the trajectories presented in Figures 6 (b)-(d) that demonstrate that as the timeslot size is increased, less and less vehicles are able to converge toward a common heading angle.

In summarizing, the results presented above demonstrate that during the interim period between communication updates, an error develops in the calculation of the distance between each vehicle and its nearest neighbour. Furthermore, Figure 9 demonstrates that due to this error, the formation control algorithm, at some point during the communication cycle, will select the wrong behavioural equation. This selection will be momentarily corrected at the end of each communication cycle when the vehicle receives an update from its nearest neighbour. However, due to the cyclical nature of the TDMA protocol, the aforementioned error will reappear during the following cycle resulting in the vehicle yet again selecting the wrong behavioural equation. Unsurprisingly, this pattern of continuously switching between the correct and incorrect behaviors will occur throughout the scenario. Consequently, as shown in Figures 10 & 11, this continuous switching between the different behaviors means that the formation control algorithm is no longer capable of ensuring that every vehicle will converge towards utilizing the orientating behaviour exclusively (Figure 11). Consequently, the formation control algorithms will instead select either the repulsive or attractive behavioural equations which, by design will result in the vehicles maneuvering in significantly different directions as demonstrated in Figure 12.

Moreover, the results demonstrate a significant reduction in the algorithm's performance as the timeslot size is increased. This is exemplified in Figure 11 where a 60% reduction in the percentage of vehicles utilizing the orientating behavioural equation is shown as a result of increasing the timeslot size from 0.5s to 8s. To further demonstrate this decline in performance, shown below in Figure 13 is the variation in the number of vehicles within each simulation able to satisfy the convergence criteria as the timeslot size increases.

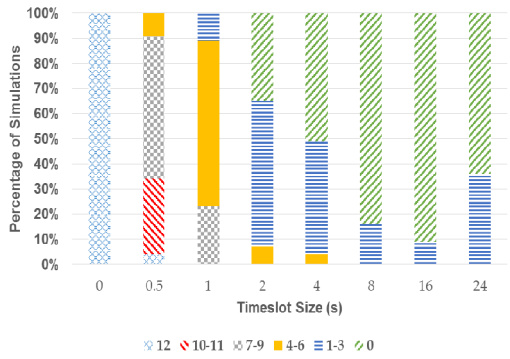


Figure 13 - Variation in the Number of Vehicles Satisfying Convergence Criteria as Timeslot Size is Increased

The results presented above demonstrate that as soon as the communication protocol is incorporated, the percentage of simulations whereby all 12 vehicles satisfy the convergence criteria drops significantly from 100% when instantaneous communication is assumed to less than 5% when the timeslot size is equal to 0.5. This value drops to zero when the timeslot size is increased further to 1s.

This deterioration is due to the fact that as the timeslot size is increased, the interim period between successive communication updates increases and as a result, the error between where the formation control algorithm estimates each vehicle to be and where they actually are, increases. As a result, since the algorithm no longer has an accurate representation of the positioning of neighbouring vehicles, it is no longer capable of selecting the correct behavioural equation and subsequently, is unable to coordinate the vehicles to form a stable group structure.

## V. Conclusions

This paper has described the implementation of a formation control algorithm that includes a realistic representation of a TDMA communication protocol utilized in the underwater environment. Furthermore, the effect that varying the timeslot size associated with this protocol from theoretically possible values through to values used in reality has been investigated. The results demonstrate that as the timeslot size increases, the error associated with the estimate of the distance between each vehicle and its nearest neighbour increases. This has the undesirable effect of resulting in the formation control algorithms selecting the wrong behavioural equation. As a result, fewer vehicles are able to converge towards utilizing the orientating behaviour which subsequently results in the vehicles being unable to manoeuvre with the same heading angle and thus, preventing the formation of a stable group structure.

Overall, the results clearly demonstrate that due to the communication constraints placed on the algorithms as a result of utilizing the TDMA protocol, the formation control algorithms, in their current state, are unable to guarantee the formation of a stable group structure.

## References


[1] D. P. Connelly, J. T. P. Copley, B. J. Murton, K. Stansfield, P. a. Tyler, C. R. German, V. Dover, L. Cindy, D. Amon, M. Furlong, N. Grindlay, N. Hayman, V. Hühnerbach, M. Judge, T. Le Bas, S. McPhail, A. Meier, K. Nakamura, V. Nye, M. Pebody, R. B. Pedersen, S. Plouviez, C. Sands, R. C. Searle, P. Stevenson, S. Taws, and S. Wilcox, "Hydrothermal vent fields and chemosynthetic biota on the world's deepest seafloor spreading centre," *Nat. Commun.*, vol. 3, p. 620, 2012.

[2] V. L. Ferrini, D. J. Fornari, T. M. Shank, J. C. Kinsey, M. A. Tivey, S. A. Soule, S. M. Carbotte, L. L. Whitcomb, D. Yoerger, and J. Howland, "Submeter bathymetric mapping of volcanic and hydrothermal features on the East Pacific Rise crest at 9??500N," *Geochemistry, Geophys. Geosystems*, vol. 8, no. 1, 2007.

[3] M. A. Moline, D. L. Woodruff, and N. R. Evans, "Optical Delineation of Benthic Habitat Using an Autonomous Underwater Vehicle," in *Journal of Field Robotics*, 2007, vol. 24, no. 6, pp. 461–471.

[4] R. B. Wynn, V. A. I. Huvenne, T. P. Le Bas, B. J. Murton, D. P. Connelly, B. J. Bett, H. A. Ruhl, K. J. Morris, J. Peakall, D. R. Parsons, E. J. Sumner, S. E. Darby, R. M. Dorrell, and J. E. Hunt, "Autonomous Underwater Vehicles (AUVs): Their past, present and future contributions to the advancement of marine geoscience," *Mar.*

*Geol.*, vol. 352, pp. 451–468, 2014.

[5] M. Bibuli, M. Caccia, and L. Lapierre, "Path-following algorithms and experiments for an autonomous surface vehicle," *IFAC Proc. Vol.*, vol. 7, no. PART 1, pp. 81–86, 2007.

[6] C. R. German, M. V. Jakuba, J. C. Kinsey, J. Partan, S. Suman, A. Belani, and D. R. Yoerger, "A long term vision for long-range ship-free deep ocean operations: Persistent presence through coordination of Autonomous Surface Vehicles and Autonomous Underwater Vehicles," *2012 IEEE/OES Auton. Underw. Veh. AUV 2012*, 2012.

[7] N. E. Leonard, D. a. Paley, F. Lekien, R. Sepulchre, D. M. Fratantoni, and R. E. Davis, "Collective Motion, Sensor Networks, and Ocean Sampling Collective Motion, Sensor Networks, and Ocean Sampling," *Proc. IEEE*, vol. 95, no. 1, pp. 48–74, 2007.

[8] S. Petillo, H. Schmidt, and A. Balasuriya, "Constructing a distributed AUV network for underwater plume-tracking operations," *Int. J. Distrib. Sens. Networks*, vol. 2012, 2012.

[9] B. Das, B. Subudhi, and B. B. Pati, "Cooperative formation control of autonomous underwater vehicles: An overview," *Int. J. Autom. Comput.*, vol. 13, no. 3, pp. 199–225, 2016.

[10] A. Marino, G. Antonelli, A. P. Aguiar, and A. Pascoal, "A new approach to multi-robot harbour patrolling: Theory and experiments," *IEEE Int. Conf. Intell. Robot. Syst.*, pp. 1760–1765, 2012.

[11] A. Birk, A.Pascoal, G.Antonelli, A.Caiti, G.Casalino, and A.Caffaz, *Cooperative Cognitive Control for Autonomous Underwater Vehicles ({CO3AUVs}): overview and progresses in the 3rd project year*, vol. 45, no. 5. IFAC, 2012.

[12] P. Bhatta, E. Fiorelli, F. Lekien, N. E. Leonard, D. Paley, F. Zhang, R. Bachmayer, R. E. Davis, D. M. Fratantoni, and R. Sepulchchre, "Coordination of an Underwater Glider Fleet for Adaptive Ocean Sampling," *Proc. Int. Work. Underw. Robot.*, no. August, 2005.

[13] C. M. Watts and E. W. McGookin, "Surge performance of an underwater vehicle with a biomimetic tendon drive propulsion system," *Proc. Inst. Mech. Eng. Part M J. Eng. Marit. Environ.*, vol. 228, no. 4, pp. 315–330, 2013.

[14] A. N. A. Mazlan and E. McGookin, "Modelling and Control of a Biomimetic Autonomous Underwater Vehicle," in *International Conference on Control, Automation, Robotics & Visions*, 2012, pp. 88–93.

[15] J. M. Anderson and N. K. Chhabra, "Maneuvering and stability performance of a robotic tuna.," *Integr. Comp. Biol.*, vol. 42, no. 1, pp. 118–126, 2002.

[16] M. Bibuli, M. Caccia, and L. Lapierre, "Development of a Two-Joint Robotic Fish for Real-World Exploration," *J. F. Robot.*, vol. 28, no. 1, pp. 70–79, 2011.

[17] T. Schmickl, R. Thenius, C. Möslinger, J. Timmis, A. Tyrrell, M. Read, J. Hilder, J. Halloy, A. Campo, C. Stefanini, L. Manfredi, S. Orofino, S. Kernbach, T. Dipper, and D. Sutantyo, "CoCoRo - The self-aware underwater swarm," in *Proceedings - 2011 5th IEEE Conference on Self-Adaptive and Self-Organizing Systems Workshops, SASOW 2011*, 2011, vol. 1, pp. 120–126.

[18] I. F. Akyildiz, D. Pompili, and T. Melodia, "Challenges for efficient communication in underwater acoustic sensor networks," *ACM SIGBED Review*, vol. 1, pp. 3–8, 2004.

[19] J. McColgan, E. McGookin, and A. N. A. Mazlan, "Analysis of the Group Structure of a School of Biomimetic AUVs Coordinated Using Nearest Neighbour Principles," in *Proceedings of the 6th International Conference on Automation, Robotics and Applications*, 2015, pp. 312–317.

[20] G. E. Burrowes, J. Brown, and J. Y. Khan, "Adaptive Space Time - Time Division Multiple Access ( AST-TDMA ) Protocol for an Underwater Swarm of AUV ' s," in *OCEANS Conference*, 2013, pp. 1–10.

[21] R. Diamant and L. Lampe, "Spatial reuse time-division multiple access for broadcast Ad hoc underwater acoustic communication networks," *IEEE J. Ocean. Eng.*, vol. 36, no. 2, pp. 172–185, 2011.

[22] E. W. McGookin and C. Watts, "A biomimetic underwater vehicle design concept," in *Further Advances in Unmanned Marine Vehicles*, London: IET, 2012, pp. 331–356.

[23] A. N. A. Mazlan, "A Fully Actuated Tail Propulsion System for a Biomimetic Autonomous Underwater Vehicle," University of Glasgow, 2015.

[24] T. I. Fossen, *Marine Craft Hydrodynamics and Motion Control*. John Wiley & Sons, Ltd, 2011.

[25] I. Aoki, "A Simulation Study on the Schooling Mechanism in Fish," *Bull. Japanese Soc. Sci. Fish.*, vol. 48, no. 8, pp. 1081–1088, 1981.

[26] I. D. Couzin, J. Krause, R. James, G. D. Ruxton, and N. R. Franks, "Collective memory and spatial sorting in animal groups.," *J. Theor. Biol.*, vol. 218, no. 1, pp. 1–11, 2002.

[27] C. K. Hemelrijk and H. Hildenbrandt, "Self-organized shape and frontal density of fish schools," *Ethology*, vol. 114, no. 3, pp. 245–254, 2008.

[28] A. Huth and C. Wissel, "The Simulation of the Movement of Fish Schools," *J. Theor. Biol.*, vol. 156, no. 1, pp. 365–385, 1991.

[29] A. Caiti, V. Calabrò, and A. Munafò, "AUV team cooperation: Emerging behaviours and networking modalities," in *IFAC Proceedings Volumes on Manoeuvring and Control of Marine Craft*, 2012, vol. 9, no. PART 1, pp. 342–347.

[30] N. Tsiogkas, Z. Saigol, and D. Lane, "Distributed Multi-AUV Cooperation Methods for Underwater Archaeology," in *MTS/IEEE OCEANS Conference*, 2015, pp. 1–5.

[31] L. Brignone, J. Alves, and J. Opderbecke, "GREX sea trials: First experiences in multiple underwater vehicle coordination based on acoustic communication," in *OCEANS 2009 - Europe*, 2009.

[32] D. M. Sotzing, C.C, Lane, "Improving the Coordination Efficiency of Limited-Commuication Multi-Autonomous Underwater Vehicle Operations Using a Multiagent Architecture," *J. F. Robot.*, vol. 27, no. 4, pp. 412–429, 2010.